Chapter 6

Characterization of the functional roles of amino acid residues in acceptor binding subsite +1 in the active site of the glucansucrase GTF180 of *Lactobacillus reuteri* 180

Xiangfeng Meng[1], Tjaard Pijning[2], Justyna M. Dobruchowska[1], Gerrit J. Gerwig[1] and Lubbert Dijkhuizen[1]

[1]Microbial Physiology, Groningen Biomolecular Sciences and Biotechnology Institute (GBB), University of Groningen, Nijenborgh 7, 9747 AG Groningen, The Netherlands,

[2]Biophysical Chemistry, Groningen Biomolecular Sciences and Biotechnology Institute (GBB), University of Groningen, Nijenborgh 7, 9747 AG Groningen, The Netherlands

Journal of Biological Chemistry, doi:10.1074/jbc.M115.687558, in press

Abstract

α-Glucans produced by glucansucrase enymes hold strong potential for industrial applications. The exact determinants of the linkage specificity of glucansucrase enzymes have remained largely unknown. Guided by the crystal structure of glucansucrase GTF180-ΔN from *Lactobacillus reuteri* 180 in complex with the acceptor substrate maltose, we identified several residues (D1028 and N1029 from domain A, as well as L938, A978 and L981 from domain B) near subsite +1 that may be critical for linkage specificity determination and investigated these by random site-directed mutagenesis. First, mutants of A978 (to L, P, F or Y) and D1028 (to Y or W) with larger side chains showed reduced degrees of branching, likely due to the steric hindrance by these bulky residues. Second, L938 mutants (except L938F) and D1028 mutants showed altered linkage specificity, mostly with increased (α1→6) linkage synthesis. Third, mutation of L981 and N1029 significantly affected the transglycosylation reaction, indicating their essential roles in acceptor substrate binding. In conclusion, glucansucrase product specificity is determined by an interplay of domain A and B residues surrounding the acceptor substrate binding groove. Residues surrounding the +1 subsite thus are critical for activity and specificity of the GTF180 enzyme, and play different roles in the enzyme function. This study provides novel insights into the structure-function relationships of glucansucrase enzymes and clearly shows the potential of enzyme engineering to produce tailor-made α-glucans

Introduction

The ability of lactic acid bacteria to produce large amounts of exopolysaccharides has drawn strong attention for industrial applications in recent years (15,16,39,46). Using sucrose as substrate, glucansucrase enzymes of lactic acid bacteria catalyze the synthesis of various α-glucans (80), which are used as biothickening agent in food industry, as plasma expander in medicine and as separation matrix in research (15,16,39,40,46). These enzymes are generally found in *Leuconostoc*, *Streptococcus*, *Lactobacillus* and *Weissella* and belong to glycoside hydrolase family 70 (GH70) (28,29). Together with enzymes from GH13 and GH77, they form clan GH-H, sharing mechanistic, structural and evolutionary characteristics (29,97,98,151). Glucansucrases catalyze reactions via an α-retaining double-displacement mechanism (28,29,97,100). First, the (α1↔2β) glycosidic linkage of the donor substrate sucrose is cleaved, resulting in the formation of a β-glucosyl-enzyme intermediate. Second, an acceptor substrate attacks the β-glucosyl-enzyme intermediate, after which the glucosyl moiety is transferred to the acceptor with retention of the α-anomeric configuration. Depending on the nature of available acceptor substrates, glucansucrases catalyze three different reactions(28,29). In the polymerization reaction, α-glucan polysaccharide is synthesized using a growing glucan chain as acceptor. The hydrolysis reaction uses water as an acceptor substrate, and sucrose is hydrolyzed into glucose and fructose. In the acceptor reaction, the glucosyl moiety is transferred to either an oligosaccharide (resulting in oligosaccharide synthesis) (134,137) or a hydroxyl-group-containing organic molecule (resulting in its glycosylation) (29,142,148).

Glucansucrases have a fully conserved catalytic center, but they produce α-glucans with different linkages, i.e. dextran with a majority of (α1→6) linkages, mutan with a majority of (α1→3) linkages, alternan with alternating (α1→6) and (α1→3) linkages and reuteran with (α1→4) and (α1→6) linkages (114). In addition, DSR-E from *Leuconostoc mesenteroides* NRRL B-1299 forms single (α1→2) glucosyl branches on dextran (47,48,199,228). Thus, all four possible linkage types between D-glucopyranosyl residues have been found in glucansucrase products. It has been proposed that their linkage specificity is determined by the orientation in which the acceptor substrate binds to the enzyme (28,88,114,151). Thus, residues forming acceptor binding subsites are expected to

be critical in determining the linkage specificity. Before the availability of structural information of glucansucrase proteins, the identification of such residues was difficult and mostly based on the sequence similarity between glucansucrases and closely related GH13 enzymes and crystal structures of the latter. The four conserved regions (I to IV) of the GH13 family enzymes, with the 3 catalytic residues and other residues interacting with donor and acceptor substrate, are also found to be present in GH70 family enzymes (28,29,97). Mutation studies thus mainly targeted residues in the four glucansucrase homology regions I-IV (24,28,88,97,151), of which some are strictly conserved while others are only moderately conserved. Indeed mutations in regions I-IV were shown to affect acceptor substrate binding and linkage specificity, confirming the roles of these residues (86,88,109,114,151,165,166). Especially, mutations in residues S1137-D1141 (GTF180 numbering) following the transition state stabilizer (D1136) in homology region IV (Fig. 1) have been shown to change the linkage compositions of synthesized α-glucan products in several gluansucrase enzymes (86,88,109,150,151,165,166).

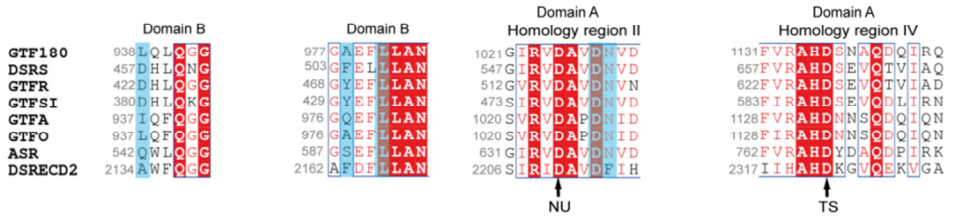

Figure 1. Partial alignment of the amino acid sequences of GH70 glucansucrase enzymes. Residues L938, A978, L981, D1028 and N1029 of GTF180 and their corresponding residues in other glucansucrase enzymes are highlighted in blue. Two amino acid residues involved in enzyme catalysis, the nucleophile residue (NU) in homology region II and transition state stabilizer (TS) in homology region IV, are indicated.

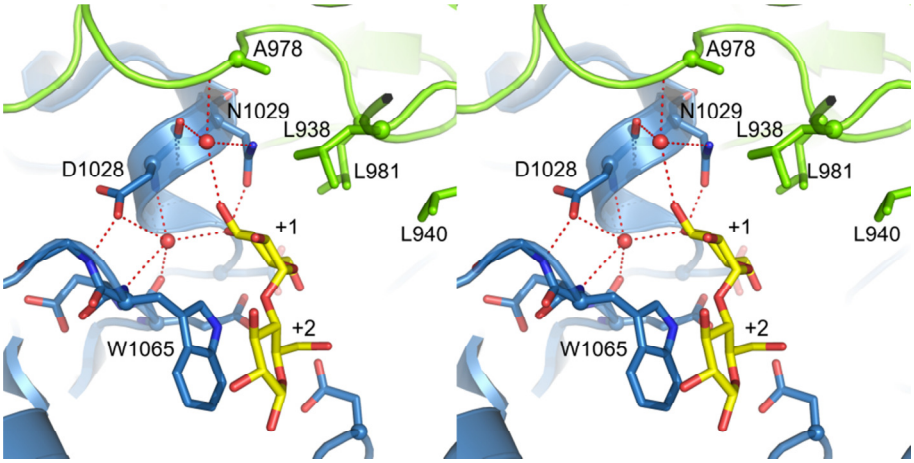

Figure 2. Stereo view of GTF180-ΔN with the acceptor maltose (yellow carbon atoms) bound in subsites +1 and +2 (PDB: 3KLL) (100). Residues N1029 and D1028 from domain A (blue) provide direct and indirect (water-mediated) hydrogen bonds to the non-reducing end glucosyl unit bound at subsite +1, respectively. Residues L938, L940, A978 and L981 from domain B (green) are also near subsite +1.

The GTF180-ΔN glucansucrase from *L. reuteri* 180 produces an α-glucan with 69% (α1→6) and 31% (α1→3) linkages, the latter being present both in the linear section as well as forming branch points (108). The elucidation of the GTF180-ΔN 3D structure provided new insights and details of donor and acceptor substrate binding in glucansucrases (100), and allowed us to expand the set of residues contributing to acceptor binding subsites, including residues outside homology regions I-IV. GTF180-ΔN has 5 domains (A, B, C, IV and V) with the active site lying at the interface of the catalytic domain A and domain B, as revealed by the protein complexes with the donor substrate sucrose (PDB: 3HZ3) and with the acceptor substrate maltose (PDB: 3KLL) (100). First, the crystal structure of the inactive mutant GTF180-ΔN D1025N bound with sucrose revealed that the seven strictly conserved residues (R1023,D1025, H1135, D1136, E1063, Y1465 and Q1509), six of them also employed by GH13 enzymes, make similar interactions with the glucosyl moiety of sucrose bound in subsite -1 (100) [nomenclature according to (229)]. Residues R1023, D1025, H1135, D1136 and Q1509 make direct H-bonds to glucosyl hydroxyl groups (100). Residue D1025 acts as the nucleophile residue which attacks the anomeric C1 carbon of the glucosyl unit of sucrose to form a β-glucosyl-enzyme covalent intermediate, stabilized by the transition state stabilizing residue (D1136). Residue E1063 is the

acid/base catalyst donating a proton to facilitate the release of fructose and depronating the acceptor molecule to activate it (100). Second, the crystal structure of GTF180-ΔN in complex with maltose revealed this acceptor substrate bound in subsites +1 and +2. At subsite +2, the residues following the transition state stabilizer (D1136) in homology region IV, which have been shown to be important for linkage specificity in previous mutagenesis studies (86,88,109,150,151,165,166), are located close to the reducing end moiety of maltose; especially residue S1137 has a direct hydrogen bond with the +2 C1 hydroxyl group (100). These observations confirmed the involvement of these residues in forming acceptor binding sites as predicted in previous studies and explain the altered linkage specificity caused by mutating these residues. At subsite +1, residues from homology regions II (D1028 and N1029) in domain A enclose the non-reducing end glucosyl moiety of maltose, providing direct and indirect hydrogen bonds with the C4 and C3 hydroxyl groups (N1029), and a water-mediated hydrogen bond with the C4 hydroxyl group (D1028) (Fig. 2) (100). Notably, in addition to these residues from the homology regions in domain A, residues from two loops in domain B (L938, L940, A978, L981) are also close to the non-reducing end glucosyl moiety in subsite +1 (Fig. 2). Due to the hydrophobic nature of their side chains they do not provide hydrogen bond interactions to the acceptor substrate molecule, but they do contribute to shaping the active site near subsite +1 (100,114). Indeed, in a recent study of dextransucrase DSRS from *L. mesenteroides* NRRL B-512F, guided by the homologous GTF180-ΔN crystal structure, several residues (including residues corresponding to residues L938, A978 and N1029 of GTF180) were targeted for combinatorial mutagenesis (115). Several of these mutants were found to display an altered product linkage distribution. Moreover, in one of our recent studies we showed that residue L940 contributes to determining linkage and reaction specificity (118); one of the mutations (L940W) even abolished synthesis of (α1→3) linkages in the products. Finally, residue W1065 has a hydrophobic stacking interaction with both the +1 and +2 glucosyl moiety of maltose. In the complex of GTF180-ΔN D1025N with sucrose it also has a direct hydrogen bond with the C1 hydroxyl group of the fructosyl moiety. It has been shown that mutating W491 of GTFI from *Streptococcus mutans* (equivalent to W1065 of GTF180-ΔN) to either glycine or alanine resulted in an enzyme devoid of detectable activity (230). Mutation of W1065 in GTF180-ΔN indeed heavily

impaired the enzyme activity (preliminary results). Therefore, we did not include W1065 mutations in the present study. Instead, residues (L938, A978, L981) of domain B and domain A (D1028 and N1029) in GTF180-ΔN were individually subjected to random mutagenesis. A large number of mutants were characterized and their α-glucan polysaccharide products were structurally analyzed, determining the linkage types distributions and their substitution pattern by NMR spectroscopy and methylation analysis, respectively. Combining the experimental results with the 3D structures of the GTF180-ΔN sucrose and maltose complexes showed that in GTF180-ΔN (a) A978 is important for the degree of branching; (b) D1028 and L938 are critical for linkage specificity, (c) L981 and N1029 are essential for the transglycosylation reaction. This study provides further insights into the structure-function relationships of GH70 glucansucrase enzymes, and offers tools to expand and control the diversity of their α-glucan products. These results were discussed in combination with previous mutagenesis studies and residues present in other glucansucrase enzymes.

Material and methods

Bacterial strains, plasmids and growth conditions

Escherichia coli DH5α (Phabagen, Utrecht, The Netherlands) was used for DNA manipulations. *E. coli* BL21 star DE3 (Invitrogen, Carlsbad, USA) was used for recombinant protein expression. *E. coli* strains were routinely grown in LB medium with the appropriate antibiotic at 37 ^{o}C. LB agar plates were made by adding 1.5% agar to the LB medium. The plasmid p15GTF180-ΔN-SX, containing N-terminally-truncated GTF180 (residue 742-1772), was used for mutagenesis and protein production (109).

Sequence alignments

Clustal Omega was used to align the amino acid sequences of GTF180 (Q5SBN3) from *L. reuteri* 180, DSRS (Q9ZAR4) from *L. mesenteroides* NRRL B-512F, GTFR (Q9LCH3) from *S. oralis* ATCC10557, GTFSI (P13470) from *S. mutans* GS 5, GTFA (Q5SBL9) from *L. reuteri* 121, GTFO (Q4JLC7) from *L. reuteri* ATCC 55730, alteransucrase ASR (Q9RE05) from *L. mesenteroides* NRRL B-1355, DSRE CD2 (Q8G9Q2) from *L. mesenteroides* NRRL B-1299. Then the

aligned sequences were submitted to EsPript for alignment based on the GTF180-ΔN crystal structure (PDB: 3KLK) (101).

Table 1. Primer pairs used for site-directed mutagenesis of *gtf180*-ΔN

Targeted Amino acid	Primer pairs (5'→3')
L938	GATTACGGTGGTNNSCAATTACAAGG
	CCTTGTAATTGSNNACCACCGTAATC
A978	AGAACTATGGTGGTNNSGAATTCTTATTAGC
	GCTAATAAGAATTCSNNACCACCATAGTTCT
L981	GGTGCGGAATTCNNSTTAGCTAATGAT
	ATCATTAGCTAASNNGAATTCCGCACC
D1028	CGAGTGGATGCTGTTNNSAATGTAGATGTTGAC
	GTCAACATCTACATTSNNAACAGCATCCACTCG
N1029	GATGCTGTTGATNNSGTAGATGTTGAC
	GTCAACATCTACSNNATCAACAGCATC

NNS: randomized codon; N: A/G/C/T; S: G/C

Site-directed random mutagenesis

Site-directed random mutagenesis was performed as previously described (118). Briefly, the Quikchange site-directed mutagenesis (Stratagene, La Jolla, California) was used to introduce mutations using primer pairs for each targeted residue (Table 1) and p15GTF180-ΔN-SX as a template. The PCR product was cleaned up with the PCR cleaning up kit (Sigma-Aldrich, St. Louis, USA) and was then transformed into *E. coli* BL21 star (DE3). After selection on LB agar plates containing 100 µg/ml ampicillin, colonies were inoculated in 96-well plates with LB medium containing 100 µg/ml ampicillin. The overnight cultures were inoculated and propagated in new 96-well plates with fresh LB medium containing 100 µg/ml ampicillin and 0.1 mM isopropy β-D-thiogalactopyranoside (IPTG) at 18 ℃ for 24 h. The cells were lysed with B-PER Protein Extraction Reagents (Thermo Scientific, Bleiswijk, The Netherlands). The supernatants obtained were used as crude enzyme extracts and were incubated with 0.1 M sucrose in 50 mM sodium acetate buffer, pH 4.5, 1 mM $CaCl_2$, at 37 ^{o}C for 15 min. The activity of each putative GTF180-ΔN mutant was monitored by measuring the release of reducing sugar with dinitrosalicylic acid reagent (224) and normalized with $OD600_{nm}$ of the corresponding culture. To reduce the probability of mutation redundancy, putative GTF180-ΔN mutants, displaying different level of activities were selected to isolate plasmid DNA, and sequenced

to verify the mutations. DNA sequencing was performed by LGC Genomics (Berlin, Germany).

Expression and purification of GTF180-ΔN mutant enzymes

Wild-type GTF180-ΔN and selected mutants were expressed using *E. coli* BL21 star (DE3) as host. Fresh LB medium was inoculated with 1% (v/v) of the overnight culture of *E. coli* BL21 star (DE3) containing the relevant plasmids and propagated to $OD600_{nm}$ 0.4-0.6. Then, the expression of enzymes was induced with 0.1 mM IPTG and cultivation was continued for 20 h at 18 ^{o}C. Cells were harvested by centrifugation (10 000 × g, 10 min). Mutant enzymes were purified as described (70). Protein concentrations were determined by reading the absorbance at 280 nm, using a NanoDrop 2000 spectrophotometer (Isogen Life Science, De Meern, The Netherlands).

Enzyme activity assays

The enzymatic activities of the different mutants were assayed as previously described (33). Briefly, the activity with sucrose was measured by the release of fructose. One unit of enzyme activity was defined as the release of 1 µmol of fructose per min. The enzymatic assay was routinely performed in 25 mM sodium acetate buffer, 1 mM $CaCl_2$, pH 4.5, at 50 ^{o}C with 30-100 nM enzymes. Samples of 25 µl were withdrawn per min (5 min in total) and inactivated with 2.5 µl 1 M NaOH. Kinetic parameters (K_m and k_{cat}) were determined using 12 different sucrose concentrations (ranging from 0.5 to 200 mM) using Michaelis-Menten kinetic equations in Sigma-Plot.

Production of α-glucans by GTF180-ΔN mutants incubated with 0.1 M sucrose

Sucrose (0.1 M) was incubated with mutant enzymes (1.0 U/ml) in 25 mM sodium acetate buffer/1 mM $CaCl_2$, pH 4.5 at 37 ^{o}C. The depletion of sucrose was verified by thin-layer chromatography (TLC). Samples (1 µl) were spotted on TLC sheets (Merck silica gel 60 F254, 20 × 20 cm). A mixture of glucose and malto-oligosaccharides (DP2 to DP7) was used as standard. The TLC plates were developed with 2-butanol:acetic acid:water = 2:1:1, and stained with orcinol/sulfuric acid. Reactions were stopped by heating at 100 ^{o}C for 10 min. Polysaccharides were isolated by adding two volumes of cold ethanol as

described previously (33). The mixtures were incubated overnight at 4 °C and the polysaccharides were collected by centrifugation (4500 × g, 20 min). The precipitated polysaccharides were washed with two volumes of cold ethanol. At the end of the reaction and before ethanol precipitation, the amount of glucose released was measured as previously described (33) and used to calculate the percentage of sucrose used for the hydrolysis reaction.

Linkage composition analysis of polysaccharides produced by mutant enzymes

The linkage composition of the polysaccharide produced by each mutant enzyme was analyzed by 500-MHz ^{1}H NMR spectroscopy and methylation analysis. ^{1}H NMR spectra were recorded on a Varian Inova Spectrometer (NMR Center, University of Groningen) at a probe temperature of 300 K. Prior to NMR analysis, samples were exchanged twice with D_2O (Cambridge Isotope Laboratories, Inc.; Andover, MA) with intermediate lyophilization and dissolved in 600 µl D_2O. Chemical shifts were expressed in ppm by reference to internal standard acetone (δ 2.225). The percentage of different linkages was estimated by integration of the respective signal peak areas.

Methylation analysis was performed as previously described (108,231). Briefly, samples of isolated polysaccharides (~5 mg) were permethylated using CH_3I and solid NaOH in Me_2SO. After hydrolysis with 2 M trifluoroacetic acid (2 h, 120 °C), the partially methylated monosaccharides were reduced with $NaBD_4$ (2 h at room temperature, aqueous solution) and neutralized by adding 4 M acetic acid. Then, boric acid was removed by co-evaporation with methanol. The mixture was acetylated with pyridine/acetic anhydride (1:1, v/v) for 30 min at 120 °C, yielding mixtures of partially methylated alditol acetates, which were analyzed by GLC-EI-MS on a GCMS-QP2010 plus instrument (Shimadzu) using a EC-1 column (30 m × 0.25 mm, Alltech) and a temperature program of 140-250 °C at 8 °C/min.

Size exclusion chromatography analysis of product mixtures

The product mixtures obtained by incubating enzymes (1.0 U/ml) with 0.1 M sucrose were first freezedried and dissolved in the eluent (DMSO with 0.05 M LiBr). Samples were incubated overnight at room temperature and then heated for 30 min at 100 ˚C. The samples were filtered through a 0.45-µm Millex PTFE

membrane (Millipore Corporation, Billerica, MA). Size exclusion chromatography analysis was performed using a SEC system (Agilent Technologies 1260 Infinity) from PSS (Mainz, Germany). The set-up consisted of an isocratic pump, an auto-sampler without temperature regulation, an online degasser, an inline 0.2 μm filter, a refractive index (RI) detector (G1362A 1260 RID, Agilent Technologies) and multiangle laser light scattering signal (SLD 7000 PSS, Mainz). As eluent, DMSO with 0.05 M LiBr was used at a flow rate of 0.5 ml/min. The samples (100 μl) were injected into a PFG guard-column and three PFG SEC columns 100, 300 and 4000 Å. Columns were thermostated at 80 ˚C and the RI detector was kept at 45 ˚C. WinGPC Unity software (PSS, Mainz) was used for data processing.

Results

Mutagenesis of GTF180-ΔN and identification of mutant enzymes

Guided by 3D protein structural information, residues L938, A978, L981, D1028 and N1029 near the acceptor subsite +1 of GTF180 were selected for mutagenesis in order to characterize their roles in enzyme function. Random mutagenesis was performed targeting these residues separately. For each targeted residue (except for L981), GTF180-ΔN inserts of eighteen active colonies were isolated for DNA sequencing in order to identify their mutations. DNA sequencing of the various selected clones resulted in identification of 24 mutants in total (Table 2). Except for L981 (only 2 mutants), a proper number of mutants for each residue (L938: 5; A978: 6; D1028: 6; N1029: 5) was obtained. However, most L981 mutations resulted in severely impaired activity and only eight active colonies were selected for DNA sequencing resulting in the identification of only two L981 mutants. When eight inactive colonies of L981 mutants were selected for further sequencing, 4 additional mutants (L981G, L981K, L981N and L981W) were found. To exclude the influence of protein expression on their activities, all mutant enzymes were expressed in *E. coli* BL21 star DE3 and purified to homogeneity as previously described (70). These mutations had no significant effect on protein expression levels. Compared to wild-type enzyme, four L981 mutants were inactive or showed very low activities (at 100 mM sucrose) (0% for L981K and L981W, <1% for L981G, <3% for L981N). Because of their low activities, these four mutants were not included in the further analysis.

A978 has an important role in branched linkage formation

^{1}H NMR analysis of the polysaccharides produced by A978 mutants (A978G, A978S, A978L, A978P, A978F and A978Y) showed that the ratio of (α1→6) and (α1→3) linkages showed no significant change compared to that of wild-type GTF180-ΔN (Table 2). In our previous study, it has been shown that the polysaccharide produced by wild-type GTF180-ΔN is built-up from five different building blocks, with different lengths of isomalto-oligosaccharides interconnected by (α1→3) linkages (Fig. 3a) (108). The (α1→3) linkages are present in both linear and branched orientation [→3)Glc*p*(1→ and →3,6)Glc*p*(1→, respectively] (Fig. 3a) (108). The relative intensity of the H-4 signal (t4, between ~ δ 3.40 and 3.45) stemming from terminal residues of α-glucan polysaccharides is an indicator for the amount of branching (Fig. 3b) (108,109,195). Examination of NMR spectra of polysaccharides produced by A978 mutants with a larger side chain (A978L, A978P, A978F and A978Y) revealed that the intensity of the t4 signal was reduced, indicating a decreased amount of branched linkages; those of A978 mutations with a small amino acid residue (A978G and A978S) did not show such a change (Fig. 3b). This change was further confirmed by methylation analysis (Table 2, chromatograms in Fig. 4 for methylation analysis). Mutation of A978 to a larger residue (L, P, F or Y) reduced the amount of branched units [→3,6)Glc*p*(1→)] to approximately half of the wild-type value. However, the (α1→3) linkages in the linear section [→3)Glc*p*(1→)] increased correspondingly, explaining the similar overall ratio of (α1→6) and (α1→3) linkages as shown by ^{1}H NMR analysis. In contrast, mutation of A978 to a smaller amino acid (G or S) had less effect on the degree of branching (Table 2, Fig. 3). All A978 mutants showed a reduced activity compared to the wild-type enzyme. Only relatively small decreases in activity were observed for mutants A978G, A978S and A978P while larger decreases were observed for mutants A978L, A978F and A978Y (Table 2). Kinetic studies revealed that the K_m values of A978G and A978F for sucrose were similar to that of GTF180-ΔN (Table 3), while their k_{cat} decreased, causing an impaired activity. The hydrolysis reactions of all A978 mutants were hardly affected, with some of them showing a slight decrease (Table 2).

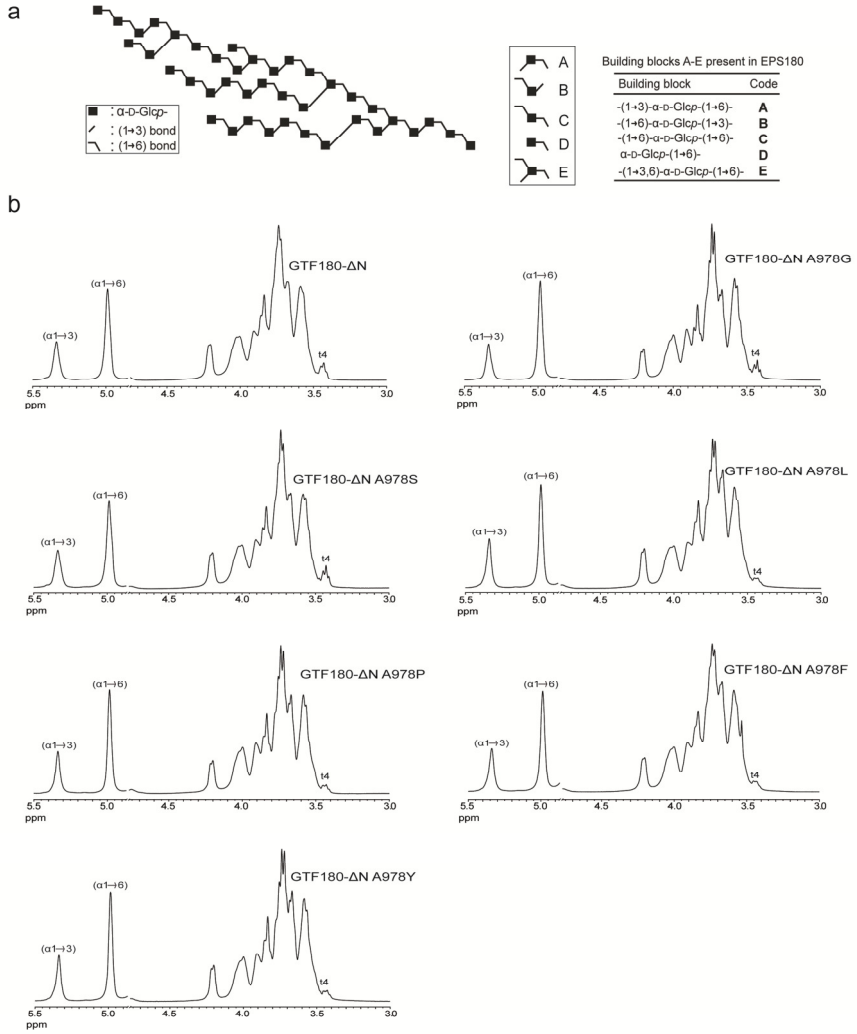

Figure 3. (a) Composite model structure of EPS180 as reported in our previous study (108). The building blocks of EPS180 are presented on the right. (b) 500-MHz 1D ^{1}H NMR spectra of the α-glucans produced by GTF180-ΔN and mutants A978G, A978S, A978L, A978P, A978F and A978Y as indicated in the figure. The H-4 signal of terminal residue (t4, between ~ δ 3.40 and 3.45), which is an indicator of branched linkages, was indicated.

L938 and D1028 are involved in linkage specificity determination

Analysis of L938 and D1028 mutants revealed a clear shift in linkage type specificity. ^{1}H NMR analysis of mutants L938A/S/K showed that the percentages of (α1→6) linkages in the α-glucan polysaccharide products increased from 67%

in the wild-type to 78%, 76% and 90%, respectively (Table 2). Methylation analysis confirmed the increase of (α1→6) linkages in the polysaccharide produced by these mutants (Table 2, L938A, L938S and L938K). Methylation analysis also revealed that the polysaccharide produced by L938K contained only 6% of branched glucopyranyl units [→3,6)Glc*p*(1→)] (as compared to 13% for the wild-type GTF180-ΔN polysaccharide products). On the other hand, the structure of α-glucan produced by mutant L938M was essentially unaffected, while α-glucan polysaccharide synthesized by mutant L938F showed a slight increase in the percentage of (α1→3) linkages.

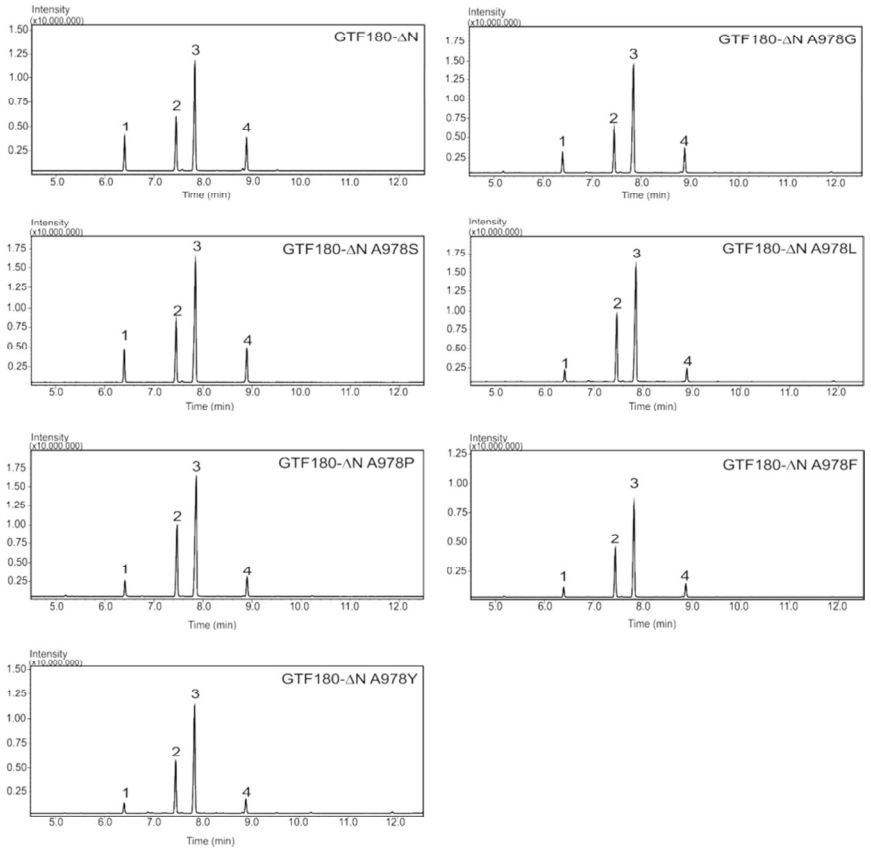

Figure 4. Methylation analysis GLC-EI-MS chromatograms of polysaccharides produced by GTF180-ΔN, A978G, A978S, A978L, A978P, A978F and A978Y as indicated in the figure. 1: [Glc*p*(1→] (1,5-di-O-acetyl-2,3,4,6-tetra-O-methylhexitol); 2: [→3)Glc*p*(1→)] (1,3,5-tri-O-acetyl-2,4,6-tri-O-methylhexitol); 3: [→6)Glc*p*(1→)] (1,5,6-tri-O-acetyl-2,3,4-tri-O-methylhexitol); 4: [→3,6)Glc*p*(1→)] (1,3,5,6-tetra-O-acetyl-2,4-di-O-methylhexitol).

Table 2. Linkage composition of polysaccharides produced, and activities of GTF180-ΔN and mutants derived

Enzymes	Methylation (%)[a]				Chemical shift (%)[b]		Relative activities[c]	Hydrolysis[e]
	Glc*p*(1→	→3)Glc*p*(1→	→6)Glc*p*(1→	→3,6)Glc*p*(1→	(α1→6)	(α1→3)		
GTF180-ΔN	11	21	55	13	67	33	100	22.2±1.3
L938A	9	12	69	10	78	22	73.7±4.2	36.6±1.6
L938S	8	15	67	10	76	24	65.2±2.0	40.9±0.8
L938F	10	32	46	12	58	42	57.5±2.6	68.2±1.2
L938K	5	7	82	6	90	10	46.3±1.7	33.6±1.5
L938M	13	23	50	14	64	36	67.4±1.5	39.3±0.9
A978F	6	27	60	7	67	33	36.9±1.3	19.7±0.9
A978S	12	20	56	12	68	32	86.9±3.0	19.8±1.0
A978G	9	18	63	10	71	29	92.9±3.2	20.2±1.8
A978L	5	30	59	6	64	36	23.5±0.5	22.5±0.8
A978P	5	28	60	7	68	32	92.3±3.5	16.7±1.5
A978Y	5	27	62	6	67	33	32.8±1.2	24.1±1.0
L981A	15	19	53	13	64	36	7.4±1.2	82.8±4.7
L981E	ND	ND	ND	ND	ND	ND	8.4±2.2	96.2±3.2
D1028Y	8	12	73	7	84	16	8.1±0.5[d]	10.0±1.3
D1028W	7	12	75	6	84	16	13.1±0.4[d]	11.8±1.4
D1028L	12	11	65	12	78	22	30.4±1.9	15.6±1.6
D1028K	13	5	70	12	82	18	7.4±0.4[d]	17.4±0.8
D1028G	13	4	71	12	85	15	31.1±1.3	12.1±0.9
D1028N	11	10	67	12	80	20	36.7±2.6	17.1±0.8
N1029Y	12	21	55	12	68	32	47.7±1.0	59.4±1.5
N1029G	ND	ND	ND	ND	42	58	16.9±1.9	74.2±3.4
N1029T	18	53	10	19	25	75	9.3±0.9	72.2±2.4
N1029M	17	39	24	20	38	62	23.5±2.1	75.7±2.6
N1029R	ND	ND	ND	ND	ND	ND	25.5±1.1	100.5±4.0

[a]The average linkage distribution data are shown in molar percentage based on GLC intensities from duplicate analysis. [b]The data represent the ratios of integration of the peak areas of the (α1→6) linkage signal at 4.99 ppm and the (α1→3) linkage signal at 5.34 ppm in the ^{1}H NMR spectra of the polysaccharides produced. [c]Average activities of three independent assays measured with 100 mM sucrose at 50 °C. The activities of all mutant enzymes were relative to that of wild-type GTF180-ΔN (100%). [d]The displayed activities were measured at 37 °C with 100 mM sucrose due to reduced stability at 50 °C. [e]Values show the percentages of sucrose used for hydrolysis of the total amount of sucrose present initially in the incubations. ND, not determined.

Substitution of D1028 with different amino acid residues (G, L, N, K, Y and W) all caused a clear increase in the percentage of (α1→6) linkages at the expense of (α1→3) linkages (Table 2). As shown by methylation analysis of the D1028G, D1028L, D1028N and D1028K mutant polysaccharides, the relative amount of 6-substituted glucopyranyl units [→6)Glc*p*(1→)] increased from 55% to 65-71% at the expense of the 3-substituted glucopyranyl unit [→3)Glc*p*(1→)], while the percentage of branched glucopyranyl units [→3,6)Glc*p*(1→)] remained almost unaffected. However, the mutations of D1028 to Y or W resulted in a significant decrease of the percentage of branched units (from 13% to 7% and 6%, respectively). The decrease of branched linkages in the polysaccharides produced

by mutants D1028Y and D1028W was also reflected by a reduced t4 signal intensity in their NMR spectra (data not shown), as observed for A978 mutants.

Besides product specificity, the relative activity was also affected. At 100 mM sucrose, mutations of D1028 had more severe effects on relative activity (down to 7-37% of wild-type activity) than mutations of L938 (down to 46-74%) (Table 2). Kinetic analysis of L938A, L938F and D1028L revealed that the major cause of their decrease in activity was a reduced k_{cat} (Table 3), since their K_m values for sucrose were hardly affected (L938A and D1028L) or showed a slight decrease (L938F) (Table 3). In addition, all L938 mutants showed an increased level of hydrolysis, up to 68.2% for L938F (Table 2). In contrast, D1028 mutants were less hydrolytic, to a varying extent (Table 2).

Table 3. Kinetic properties of wild-type GTF180-ΔN and mutants derived

Enzymes	K_m (mM)[b]	k_{cat} (s^{-1})[b]	k_{cat}/K_m (s^{-1} mM^{-1})
GTF180-ΔN[a]	5.0±0.3	303.0±3.6	60.6
L938A	5.7±0.4	212.7±4.4	37.3
L938F	2.8±0.2	165.1±5.7	59.0
A978G	4.8±0.2	259.5±3.7	54.1
A978F	5.4±1.1	88.9±2.9	16.5
L981A	38.4±4.2	31.1±2.6	0.8
D1028L	4.4±0.3	85.2±3.8	19.4
N1029Y	2.9±0.2	136.5±3.2	47.1

[a]Data from previous study (118). [b]The kinetic parameters (K_m for sucrose and k_{cat}) were determined with 12 different sucrose concentrations ranging from 0.5 mM to 200 mM.

L981 and N1029 are essential for transglycosylation

Mutants L981A and L981E retained only 7.4% and 8.4% activity, respectively, at 100 mM sucrose. Kinetic analysis of L981A showed that both its K_m and k_{cat} were affected significantly, resulting in a very low catalytic efficiency (Table 3). Product analysis of L981A and L981E showed that their relative amount of hydrolysis increased significantly to 82.8% and 96.2%, respectively (Table 2), indicating that they prefer to use water as acceptor substrate. L981E hardly produced any polysaccharides while L981A produced minor amounts of polysaccharide. As shown by ^{1}H NMR and methylation analysis, the structure of the α-glucan polysaccharide produced by mutant L981A was similar to that of wild-type GTF180-ΔN (Table 2). To conclude, L981 mutations significantly

impaired the enzyme activity and affected the reaction specificity of the enzyme, shifting the reaction balance to hydrolysis (L981A and L981E).

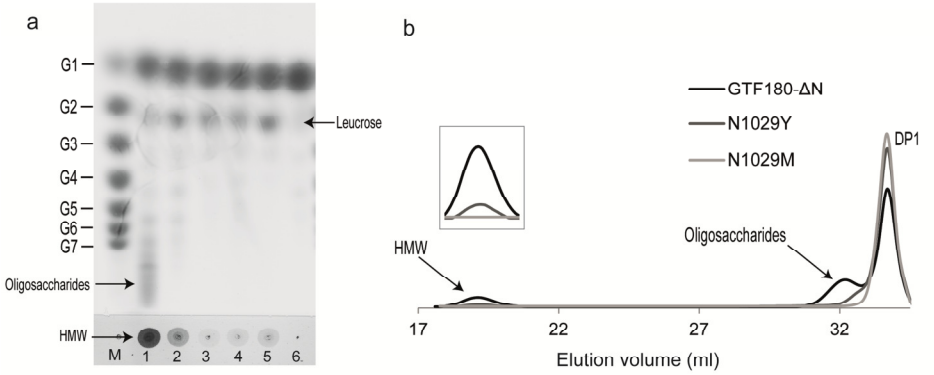

Figure 5. (a) TLC analysis of products formed from incubation of GTF180-ΔN and N1029 mutants (1.0 U/mL) with 0.1 M sucrose in 25 mM NaAC/1 mM $CaCl_2$ buffer, pH 4.5 at 37 ^oC. A mixture of glucose (G1) to maltoheptaose (G7) was used as standard (M). 1: GTF180-ΔN, 2: N1029Y, 3: N1029G, 4: N1029T, 5: N1029M, 6: N1029R. (b) Size exclusion chromatography analysis of product mixtures obtained by incubating 1.0 U/ml GTF180-ΔN, N1029Y and N1029M with 0.1 M sucrose in 25 mM NaAC/1 mM $CaCl_2$ buffer, pH 4.5 at 37 ^oC . HMW: high molecular weight polysaccharides.

Substitution of N1029 by various other residues (G, T, M, R and Y) strongly increased the hydrolysis, especially for N1029R (Table 2). N1029Y still catalyzed the synthesis of polysaccharide from sucrose (Fig. 5). NMR and methylation analysis showed that the polysaccharide produced by N1029Y was not significantly different compared to that of wild-type GTF180-ΔN. All the other N1029 mutants produced virtually no polysaccharides (Fig. 5). Using sucrose as substrate, N1029G, N1029T and N1029M catalyzed the synthesis of a small amount of short oligosaccharides (mainly leucrose). NMR analysis of the very low amounts of ethanol-precipitable polymeric material obtained with these mutant enzymes showed an increased amount of ($\alpha 1 \rightarrow 3$) linkages (from 58% to 75%), indicating that N1029 is also involved in determination of linkage specificity. Most N1029 mutants showed a relatively low activity (Table 2). Kinetic analysis of mutant N1029Y indicated a slightly decreased K_m (2.9 mM) and a clearly reduced k_{cat} (136.5 s^{-1}) (Table 3). Thus this mutant enzyme can still efficiently bind the substrate sucrose, and its relatively low activity is mainly caused by a reduced k_{cat}.

Discussion

Although the linkage specificity determinants of glucansucrase enzymes have been the focus of research in several studies, they are still not fully understood. Initially, amino acid residues that were important for linkage specificity determination were identified by primary sequence alignment with GH13 family enzymes, which have been studied extensively and their crystal structures are available (88,151). For example, the tripeptide following the transition state stabilizer (D1136) varies among different glucansucrases (Fig. 1) (86,88,109,151). GTF180 contains SNA at this position; mutations targeting these residues altered linkage specificity of GTF180 and even introduced a third type of linkage [(α1→4) linkage] not present in the α-glucan produced by wild-type enzyme (86,88,108-110,151). The corresponding tripeptide in the dextransucrase DSRS (SEV) has been the subject of mutation studies (88,115). GTFR from *Streptococcus oralis* producing mainly (α1→6) linked α-glucan, and GTFSI from *Streptococcus mutans* producing mainly (α1→3) linkages have the same tripeptide as DSRS. Reuteransucrases GTFA and GTFO [synthesizing (α1→4) and (α1→6) linkages] contain an NNS tripeptide while alternansucrase ASR producing an α-glucan with alternating (α1→6) and (α1→3) linkages has YDA. In all cases, the tripeptide has been shown to be important for linkage specificity determination in the respective glucansucrases (86,88,109,115,150,151). Likewise, the fourth and fifth residue following the transition state stabilizer have been targeted for mutagenesis studies and were demonstrated to be critical for linkage specificity (109,165,166). The available crystal structures of glucansucrases showed that residues following the transition state stabilizer are close to the +2 acceptor subsite, thus explaining their effects on linkage specificity. However, while the above described residues are in domain A, the crystal structure of GTF180-ΔN in complex with maltose revealed that the acceptor binding site is shaped by residues not only from domain A but also from domain B (100). Thus, the latter may also contribute to acceptor binding and linkage specificity. For example, our previous study, targeting residue L940 from domain B of GTF180-ΔN, showed that it is critical for linkage specificity (118). Surprisingly, mutation L940W completely abolished (α1→3) linkage synthesis and only synthesized (α1→6) linkages (118). This residue shows limited

variations among glucansucrases; in reuteransucrase GTFA and GTFO, and DSRE CD2 producing (α1→2) linkages, it is replaced by phenylalanine.

In our present study, we show that other residues from domain B (L938, L981, A978) and domain A (D1028 and N1029) of GTF180-ΔN are also critical for linkage specificity and activity. First, The polysaccharides produced by A978 mutant enzymes showed no significant changes in overall ratio of (α1→6) and (α1→3) linkages. Nevertheless, our detailed structural analysis showed that this residue is important for branched linkage formation, reflected by the reduced amount of branched linkages in the polysaccharides produced by A978 mutant enzymes with larger side chains (L, P, F, Y). These results may be explained by inspection of the GTF180-ΔN-isomaltotriose complex model (Fig. 6) (100). In this model, residue A978 is located near subsite +II' with its main chain nitrogen hydrogen bonded to the C3 hydroxyl group of the +II' glucosyl moiety. Mutating A978 to a large residue may partially block the + II' subsite and disfavor formation of branched linkages. Such mutations of A978 may also invoke local conformational changes, possibly involving the protein main chain. The observed adverse effects on the synthesis of branched linkage may thus be a result of steric effects near subsite +II' as well as the loss of hydrogen bond interactions with acceptor substrates. Thus, residue A978 of GTF180 is the first glucansucrase residue identified to be clearly involved in branch formation. Amino acid sequence alignment analysis of different glucansucrase enzymes showed that in DSRS, which produces less branched linkages in its polysaccharide compared to GTF180, the corresponding residue is a phenylalanine. However, A978 is replaced by Y, Y and Q in GTFR, GTFSI and GTFA respectively, which still produce relative high amounts of branches (70,86,102); this indicates that the residue at this position may play different roles in different glucansucrase enzymes. Mutant A978G and A978F showed no significant change in their K_m values for sucrose, which can be explained by the fact that in the GTF180-ΔN sucrose complex (PDB: 3HZ3), residue A978 is far (≈11 Å) from the +1 fructosyl moiety of sucrose. The impaired activity of mutants can thus be explained by the observed decrease in k_{cat}. Mutations of A978 had no effect on sucrose binding, however, it did affect acceptor substrate binding, as shown above.

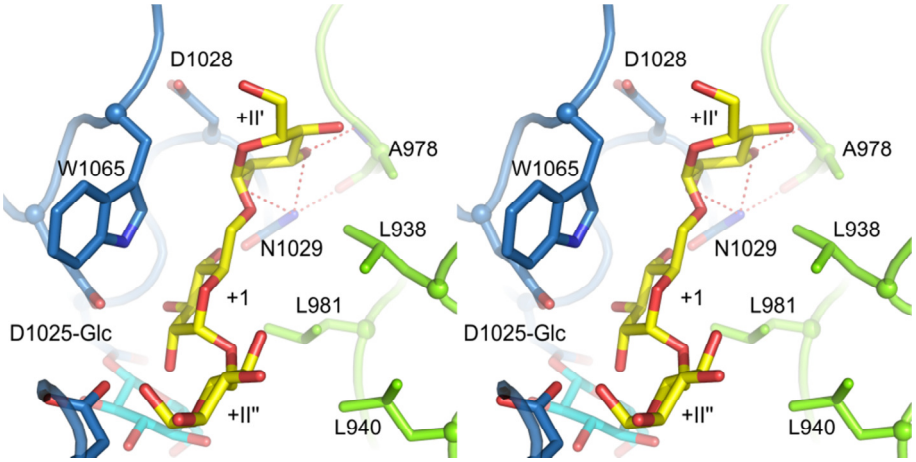

Figure 6. Stereo view of docked isomaltotriose in the active site of modeled GTF180-ΔN glucosyl-enzyme intermediate (100). Residues from domain A (blue) and B (green) surrounding the +1 and +II' subsites are indicated, including those (D1028, N1029, L938, A978 and L981) mutated in this study.

The observed effects of L938 mutations in GTF180-ΔN for linkage specificity may be explained by the fact that this residue is located in the N-terminal part of domain B, and contributes to shaping the groove near the catalytic site (29,100), with the +1 glucosyl moiety of maltose bound between W1065 on one side and L938 and L981 on the other side (Fig. 2). Mutating L938 to methionine (similar in size and properties to leucine) hardly affected the linkage composition. However, mutation to alanine or serine, both smaller than the wild-type leucine, increased the amount of (α1→6) linkages. The long and positively charged side chain of lysine in mutant L938K may disfavor the acceptor binding mode necessary for the formation of (α1→3) branches. On the other hand, the bulky and neutral aromatic side chain of phenylalanine in mutant L938F does not show such an effect, indicating that not only size but also charge may play a role. Together, the results show that mutations in L938 affect the linkage specificity of GTF180-ΔN, depending on the size and physicochemical properties of the amino acid side chain introduced.

Residue L981 is located in the same N-terminal loop of domain B as A978, delineating the sucrose binding pocket. However, it is much closer (≈4 Å) to the sucrose binding site. Moreover, L981 is strictly conserved in all the glucansucrase enzymes, suggesting an important role for this residue. Our mutational results

with L981 in GTF180-ΔN confirmed this; all mutants showed a heavily impaired activities. Mutations in L981 probably impaired the substrate binding causing low activity (L981A, L981E, L981G and L981N) or even inactivation of the enzyme (L981K and L981W). In addition, the ratio of hydrolysis of mutants L981A and L981E was significantly increased, suggesting that L981 is also essential for transglycosylation.

Our mutation studies show that D1028 affect (α1→6) and (α1→3) linkage synthesis and is also involved in branched linkage formation. Residue D1028 is part of homology region II and is highly conserved in glucansucrases. In the GTF180-ΔN maltose complex (PDB: 3KLL), it is involved in a hydrogen bond network around subsite +1 formed by residues D1028, N1029 and W1065, and makes a water-mediated hydrogen bond to the C4 hydroxyl group of the non-reducing end glucosyl unit, which is in a productive orientation to form an (α1→6) linkage (Fig. 2) (100). Thus, the observed effects of D1028 mutations on (α1→6) and (α1→3) linkage synthesis are likely due to changes in the interactions possible with acceptor substrates at subsite +1, disfavoring (α1→3) linkage synthesis. In docking studies with wild-type GTF180-ΔN, isomaltotriose was observed to bind such that its middle glucosyl unit is oriented in favor of (α1→3) branch formation (Fig. 6) (100). In this model, residue D1028 is close (within 5 Å) to the non-reducing-end glucosyl moiety at the +II' subsite (Fig. 6). For mutations involving a large aromatic side chain, the decrease of branched (α1→3) linkage synthesis indicates that steric effects play a role, as these bulky residues may partially block the + II' subsite (Fig. 6). All N1029 mutants showed the significantly increase of the ratio of hydrolysis and (α1→3) linkage synthesis in their α-glucan products (except N1029Y). In the GTF180-ΔN complexes with sucrose and maltose, residue N1029 is involved in a hydrogen bond network, making indirect or direct hydrogen bonds with the sugar moiety in subsite +1 (fructosyl or glucosyl, respectively; Fig. 2), explaining its involvement in the determination of reaction and linkage specificity. N1029 is part of homology region II and is highly conserved in glucansucrases (Fig. 1), confirming its importance in glucansucrase function. Since glucansucrases producing different linkages contain the same residue in positions 1028-1029 (except for DSRECD2), these two residues are probably not specific residues that determine the difference of linkage specificity in these glucansucrases.

Together, these mutagenesis studies showed that the glucansucrase linkage specificity is not determined by one or a few amino acid residues. Instead, it is determined by an interplay of different amino acid residues from both domain A and domain B. Together, these residues shape the acceptor binding sites and create the specifict micro-physicochemical environment; thus determines which hydroxyl group of the non-reducing end glucosyl moiety of an acceptor substrate is capable of attacking the glucosyl-enzyme intermediate to form the corresponding linkage type. This interplay explains why, even with different amino acid residues at a certain position, different glucansucrases still may have similar linkage specificities and the glucansucrases containing identical amino acid residues in the specific positions descried above synthesize different products. Although the contribution of different residues complicates the rationalization of acceptor specificity in glucansucrases, our present study shows that 3D structure guided mutagenesis is an effective approach for changing the linkage specificity of glucansucrase enzymes and producing novel α-glucans. On the other hand, combinatorial mutagenesis (involving several residues at the same time) represents an alternative, outstanding approach to diversify the linkage composition of α-glucans produced. Recently, such a combinatorial mutagenesis approach, covering several residues from both domain A and domain B, was applied to DSRS from *L. mesenteroides* NRRL B-512F making use of the NMR-based high-through-put screening carbohydrate active enzyme specificity method (115,232). Indeed, obtained mutants produced a range of novel α-glucans with an altered relative amount of (α1→3) linkage (3-20%) (164). The ultimate goal of glucansucrase mutation studies would be to have glucansucrase mutants produce tailor-made α-glucans with desired linkage type distribution, by creating the acceptor substrate binding site with appropriate physicochemical microenvironment. With current insights, this goal is still beyond reach. Our current study contributes to a better understanding towards the linkage specificity, especially for branched linkage formation, in relation to the 3D structure of the acceptor binding sites.

Conclusions

This paper reports the 3D structure-guided identification and mutation of amino acid residues around subsite +1 in GTF180-ΔN, some of which are outside the homology regions I-IV that previously have been targeted. Using mutagenesis,

we changed the relative amounts of linkage types (increase of (α1→6) linkages in L938 and D1028 mutants), changed the balance between (α1→3) linkages in the linear section and branched (α1→3) linkages (several A978 mutants), or shifted the reaction balance to hydrolysis (L981 and N1029 mutants). Analysis of these results combining those of previous mutagenesis studies, it makes it evident that the interplay of residues from both domain A and domain B, forming acceptor binding site determines the catalytic activity, reaction and linkage specificity of the glucansucrase enzymes. This study provides novel insights into the structure-function relationship of glucansucrases and clearly shows the potential of enzyme engineering for the synthesis of tailor-made α-glucans.

Acknowledgements

This work was financially supported by the China Scholarship Council (XM), and by EU project NOVOSIDES FP7-KBBE-2010-4-265854 (LD). We acknowledge the strong support of Prof. Johannis P. Kamerling in writing the manuscript. We thank Albert Woortman (Macromolecular Chemistry and New Polysaccharide Materials, University of Groningen) for assistance in size exclusion chromatography analysis of α-glucan products.